

!

!

!

!

!

!

!

!

!

Chapter I

Introduction

!

!

!

CHAPTER-I
INTRODUCTION

Sr. No.	Contents	Page No.
1.1	General	1
	1.1.1 Challenges	2
	1.1.2 Aims and objectives	2
1.2	Literature Review	3
	1.2.1 Transparent Conducting Oxides (TCOs)	3
	1.2.2 Developments in TCOs	3
	1.2.3 ZnO as a TCO material	6
	1.2.4 Spray pyrolysis deposited ZnO thin films	7
1.3	Properties of Zinc oxide (ZnO)	13
	1.3.1 Structural properties	13
	1.3.2 Physical properties	15
	1.3.3 Mechanical properties	16
	1.3.4 Optical properties	16
	1.3.5 Electrical properties	19
1.4	Applications of ZnO	19
1.5	Donor and Acceptor levels in ZnO	21
	1.5.1 Donor (<i>n</i> -type) levels	21
	1.5.2 Acceptor (<i>p</i> -type) levels in ZnO	22
1.6	Organization of thesis	24
	References	25

1.1 General

So much of the academic literature on transparent conductive oxides (TCOs) films prepared by a spray pyrolysis deposition (SPD) method is focused on indium-tin-oxide (ITO) and fluorine-tin-oxide (FTO) thin films. However in recent years, due to their wide applications, the cost of ITO and FTO TCOs is rising experimentally and there by many scientists engaged in searching new kind of materials. Of these, ZnO thin films have attracted the most attention, because unlike to the more commonly used ITO, ZnO is a non-toxic, inexpensive and abundant in nature. We can find obvious evidence in the fact that more than 2500 research papers have been published on ZnO thin films prepared by different methods and envisaged in various applications from the physical, chemical, electrical, optical, morphological and structural aspects.

Zinc oxide (ZnO) is II-VI compound *n*-type semiconductor having a band gap of 3.37 eV at room temperature, large exciton binding energy (60 meV) and optical transparency [1, 2]. The properties of ZnO with a direct band gap and high exciton binding energy are much higher than those of other widely used wide-band-gap materials, for example, ZnSe (20 meV) and GaN (21 meV), etc. Moreover, the ZnO thin films can be deposited at a lower temperature than ZnSe and GaN. Therefore, its wide-band-gap energy were useful in short-wavelength optoelectronic devices, such as UV lasers, blue to UV light-emitting diodes and UV detectors, etc. [3, 4], which can be applied to high density data storage systems, solid-state lighting, secure communications and bio-detection.

The growth methods of ZnO thin films have been considered in literature include pulsed laser deposition [5,6], thermal evaporation [7], chemical vapor deposition [8], metal oxide chemical vapor deposition [9], sol-gel [10], magnetron sputtering [1,11,12], and spray pyrolysis, etc., [13-15] for designing transparent and conducting ZnO thin films. However, very few of them have been succeeded in achieving both transparent and conducting behaviors. Additionally, thin films deposited by spray pyrolysis deposition (SPD) can result in better crystal structure at higher temperature than by other techniques, which is caused by the higher energy of the ablated particles in the laser-produced plasma plume. Moreover, there are still other advantages of using the SPD technique making it so effective. For example, deposition processes in controllable oxygen ambient pressure result in high controllability of thin film chemical element composition and grain growth processes. Thus, in this work, as-deposited and doped ZnO thin films by SPD techniques are studied with the influence of film growth conditions, such as substrate temperature, ambient air flow pressure,

concentration of precursor and the volume of precursor on the structural, optical and electrical properties of ZnO thin films etc.

1.1.1 Challenges

High quality transparent and conducting ZnO thin films can be deposited by SPD method under certain process conditions, but, it is well-known that different process machines or different ZnO targets would make the conditions a little different, sometimes totally different. Therefore, for understanding a new material (ZnO) and new low-cost equipment as such SPD, initially we should systematically arrange a series of experiments to find out the relative optimized SPD conditions. For investigating the influence of different parameters of SPD on ZnO and doped ZnO thin films, in each experiment only one parameter is varied by keeping others at the same level. If there is any change in the parameters of SPD, the experiment should be done all over again. To commercialize ZnO is each researcher's purpose, but the electrical properties of ZnO are always relatively weaker compared with ITO and FTO.

Therefore, in proposed work, it is planned to dope the pure ZnO with boron (B) and nitrogen (N) and also their co-doping in order to grow a low resistive and highly transparent ZnO thin films. For achieving the optimized ZnO along with boron doped, nitrogen doped and boron nitrogen co-doped ZnO thin films, series of experiments to optimize the SPD parameters were rearranged.

1.1.2 Aims and objectives

I. The development and deposition of ZnO thin films by using a simple, reproducible, energy intensive and low-cost deposition technique is an important strategy in achieving the low-cost, highly conductive ZnO thin films.

II. It is an endeavor to study the structural, optical, surface morphological, compositional, etc., properties of ZnO and B-N co-doped ZnO thin films deposited by spray pyrolysis method.

III. To optimize the SPD technique with ZnO thin films for conductivity and optical transparency by varying airflow rate, precursor concentration, quantity of precursor and substrate temperature.

IV. To investigate the influence of airflow rate, precursor concentration, quantity of precursor and substrate temperature on ZnO thin films.

V. To investigate the influence B and N doping on ZnO thin films with respect to conductivity and optical transparency by varying precursor concentration and substrate temperature.

VI. To investigate the influence B-N co-doping on ZnO thin films with respect to conductivity and optical transparency by varying precursor concentration and substrate temperature.

1.2 Literature Review

1.2.1 Transparent Conducting Oxides (TCOs)

Transparent conductors (TCs), both oxides and non-oxides including single layer and multilayer sandwiched structures, have been investigated for transparent or semitransparent as the case may be, conducting electrode applications in optoelectronic devices such as solar cells, liquid crystal displays, and light emitting diodes owing to their desirable properties such as electrical conductivity and optical transparency [16]. Meanwhile, doped metal oxide-based thin film TCO's with much better transmittance, as compared to the all metal varieties, have been and continue to be developed. Electrical conduction in TCOs is achieved by introducing native defects (i.e., oxygen vacancies) or by doping (typically with higher or lower -valence elements). Currently, the carrier concentration in well-developed TCOs varies from 10^{20} to 10^{21} cm^{-3} . By taking advantage of TCOs common nature of possessing high optical transmittance and electrical conductivity, low series resistance can be achieved without obstructing light emission or absorption, depending on the application.

The optical transparency and electrical conductivity in these materials depend on the nature, number, and atomic arrangements of metal cations in crystalline or amorphous oxide structures, surface morphology, and the presence of intrinsic or intentionally introduced defects. Minami *et al.* [17] reviewed the status and prospects for further development of polycrystalline or amorphous TCO thin films for transparent electrode applications. A recent review of TCO materials by Exarhos and Zhou [18] discusses processing approaches, presents a microscopic description of electronic conductivity in transparent metal oxide systems, and offers guidelines for the design and subsequent development of new materials.

1.2.2 Development in TCOs

The first realization of a TCO material occurred slightly more than a century ago when a thin film of sputter deposited cadmium (Cd) metal underwent incomplete thermal oxidation upon post deposition by heating in air [19]. Revelations dating back to about 1960s that ITO,

a compound of indium oxide (In_2O_3) and tin oxide (SnO_2), exhibits both excellent electrical and optical properties [20, 21] paved the way for extensive studies on this material family. In_2O_3 has a bixbyite-type cubic crystal structure, while SnO_2 has a rutile crystal structure and both of them are weak n -type semiconductors. Their charge carrier concentrations and thus, the electrical conductivities are strongly increased by extrinsic dopant which is anticipated [22, 23]. The reported dopants for In_2O_3 -based binary TCOs include Sn, Ge, Mo, Ti, Zr, Hf, Nb, Ta, W, Te, and F, etc. [24] as well as Zn [25]. The In_2O_3 -based TCOs doped with the aforementioned impurities were found to possess very good electrical and optical properties. The laboratory resistivity of Sn-doped In_2O_3 (ITO) film was about $1 \times 10^{-4} \Omega\text{-cm}$ [17]. As noted above, despite the nomenclature of Sn-doped In_2O_3 (ITO), this material is really an In_2O_3 -rich compound of In_2O_3 and SnO_2 . SnO_2 is a semiconductor with a band gap of 3.62 eV at 298 K and is particularly interesting because of its low electrical resistance coupled with its high transparency in the UV-visible region [26, 27]. Fluorine (F), antimony (Sb), niobium (Nb), and tantalum (Ta) are most commonly used to achieve high n -type conductivity while maintaining high optical transparency [28-31].

FTO is the second widely used TCO material, mainly in solar cells due to its better stability in hydrogen-containing environment and at high temperatures required for device fabrication. The typical value of FTO's average transmittance is about 80% [31, 32-35]. However, electrical conductivity of FTO is relatively low [31] and it is more difficult to pattern *via* wet etching as compared to ITO [36]. In short, more efforts are beginning to be expended for TCOs by researchers owing to their abovementioned uses spurred by their excellent electrical and optical properties in recently popularized devices.

In addition to ITO and FTO, ZnO as a TCO, turning attention of researcher to upcoming alternative due to previously mentioned merits. ZnO with an electron affinity of 4.35 is typically an n -type semiconductor material with the residual electron concentration of $\sim 10^{19} \text{ cm}^{-3}$ [37]. However, the doped ZnO films have been realized with very attractive electrical and optical properties for electrode applications. The dopants that have been used for the ZnO-based binary TCOs are Ga, Al, B, In, Y, Sc, V, Si, Ge, Ti, Zr, Hf, and F, etc. [20]. Among the advantages of the ZnO-based TCOs are low cost, abundant and non-toxicity [38].

At present, ZnO heavily doped with Ga and Al (dubbed GZO and AZO) has been demonstrated to have low resistivity and high transparency in the visible spectral range and, in some cases, even outperform ITO and FTO. The dopant concentration in GZO or AZO can

reach conductivity up to 10^{20} – 10^{21} cm^{-3} and although mobility near $95 \text{ cm}^2/\text{V}\cdot\text{s}$. In GZO film typical reported mobility is near or slightly below $50 \text{ cm}^2/\text{Vs}$ [12]. Ionization energies of Al and Ga donors (in the dilute limit which decreases with increased doping) are 53 and 55 meV, respectively, which are slightly lower than that of In (63 meV) [39]. Agura *et al.* [40] reported a very low resistivity of $\sim 8.5 \times 10^{-5} \Omega\cdot\text{cm}$ for AZO, and Park *et al.* reported a resistivity of $\sim 8.1 \times 10^{-5} \Omega\cdot\text{cm}$ for GZO [41], both of which are similar to the lowest reported resistivity of $\sim 7.7 \times 10^{-5} \Omega\cdot\text{cm}$ for ITO [42]. The typical transmittance of AZO and GZO is easily 90% or higher [43-45].

Table 1.1: Physicals, electrical and optical properties and synthesis methods of TCO material thin films. (* - unavailable)

TCO	Deposition techniques	Band gap (eV)	Carrier concentration (10^{19} cm^{-3})	Mobility ($\text{cm}^2/\text{V s}$)	Resistivity ($10^{-4} \Omega\text{cm}$)	Transmittance (%)
ITO [46]	Commercial	*	*	*	1–1.9	*
ITO [47]	PLD	*	13.8	53.5	0.845	>80
ITO [48]	Spray pyrolysis	*	18	40	0.95	81
ITO [49]	Sputtering	3.78–3.80	14.6–18.9	25.7–32.7	1.28–1.29	≥ 80
FTO [50]	Spray pyrolysis	4.12–4.18	1.02–9.59	11.1–18.9	*	≥ 75
FTO [51]	Spray pyrolysis	*	24.9	6.59	3.8	*
FTO [51]	Spray pyrolysis	3.15–3.	4.5–7	12–24	3.85–7.51	~ 80
FTO [53]	CVD	*	3.05	19	10.9	~ 80
AZO [54]	MBE	*	2.1	57		*
AZO [55]	CVD	3.59	8.7	*	*	*
AZO [56]	SoI-gel	*	2.5	31	1.2	>90
AZO [57]	Sputtering	*	~ 5.5	67	1.4	*
AZO [58]	Sputtering	*	15	22	1.9	>80
AZO [59]	Sputtering	*	9	25	2.7	>85
AZO [60]	Sputtering	3.18–3.36	*	*	980	>85
AZO [61]	PLD	*	13.1	36.7	1.3	89–95
AZO [62]	PLD	*	15	47.6	0.85	>88
AZO [63]	PLD	3.51–3.86	20.2	16.2	1.91	75–90
GZO [64, 65]	MBE	*	8.1	42	1.9	>80
GZO [66, 67]	MBE	*	3.5–15	18–40	≥ 1.9	>90
GZO [68]	CVD	*	*	*	1.2	>85
GZO [69]	Sputtering	3.37–3.43	1–6	5–35	5.3	~ 90
GZO [70]	PLD	3.51	146	30.96	0.812	>90
GZO [71]	PLD	*	64	4.9	2.6	>90

Table 1.2: History of dopants and deposition processes used for obtaining doped TCOs.

Material	Process	Reference
SnO ₂ :Sb	Spray pyrolysis	J. M. Mochel (Corning), 1947[72]
SnO ₂ :Cl	Spray pyrolysis	H. A. McMaster (Libbey-Owens-Ford), 1947 [73]
SnO ₂ :F	Spray pyrolysis	W. O. Lytle and A. E. June (PPG), 1951 [74]
In ₂ O ₃ :Sn	Spray pyrolysis	J. M. Mochel (Corning), 1951 [75]
In ₂ O ₃ :	Sputtering	L. Holland and G. Siddall, 1955 [76]
SnO ₂ :Sb	CVD	H. F. Dates and J. K. Davis (Corning), 1967 [77]
Cd ₂ SnO ₄	Sputtering	A. J. Nozik (American Cyanamid), 1974 [78]
Cd ₂ SnO ₄	Spray Pyrolysis	A. J. Nozik (American Cyanamid), 1976 [79]
SnO ₂ :F	CVD	R. G. Gordon (Harvard), 1979 [80]
TiN	CVD	S. R. Kurtz and R. G. Gordon (Harvard), 1986 [81]
ZnO:In	Spray Pyrolysis	S. Major <i>et al.</i> (Indian Ist. Tech), 1984 [82]
ZnO:Al	Sputtering	T. Minami <i>et al.</i> (Kanazawa), 1984 [83]
ZnO:In	Sputtering	S. N. Qiu <i>et al.</i> (McGill), 1987 [84]
ZnO:B	CVD	P. S. Vijayakumaret <i>al.</i> (Arco Solar), 1988 [85]
ZnO:Ga	Sputtering	B. H. Choi <i>et al.</i> (KAIST), 1990 [86]
ZnO:F	CVD	J. Hu and R. G. Gordon (Harvard), 1991 [87]
ZnO:Al	CVD	J. Hu and R. G. Gordon (Harvard), 1992 [88]
ZnO:Ga	CVD	J. Hu and R. G. Gordon (Harvard), 1992 [89]
ZnO:In	CVD	J. Hu and R. G. Gordon (Harvard), 1993 [90]
Zn ₂ SnO ₄	Sputtering	H. Enokiet <i>al.</i> (Tohoku), 1992 [91]
ZnSnO ₃	Sputtering	T. Minami <i>et al.</i> (Kanazawa), 1994 [92]

1.2.3 ZnO as a TCO material

Among all the TCO materials such as ITO, FTO, binary and ternary, the ZnO emerged as a good TCO material with various intrinsic and extrinsic dopants and good electrical, optical properties. B-doped ZnO film has been reported to exhibit laser-induced photo-voltage (LPV), which is expected to make it a candidate for position sensitive photo-detectors [93]. Indium (In)-doped ZnO thin films prepared by using pulsed laser deposition and spray pyrolysis method for TCO applications [94, 95], respectively. Y-doped ZnO deposited by sol-gel method on silica glass [96] and Ilicanet *al.* [97] reported on the

structural, optical and electrical properties of F-doped ZnO formed by the sol-gel process. It is interesting to note that nanostructures such as nanorods [98] and nanotips [99] as well as controllable surface roughness [100] could enhance light extraction/absorption in optoelectronic devices, thus improving the device performance. Fortunately, various nanostructures can be easily achieved in ZnO by choosing and controlling the growth conditions, temperatures, concentrations and capping agents, etc. One disadvantage of ZnO-based TCOs is that they degrade at the faster than ITO and FTO when exposed to damp and hot environment [99].

In addition to those above-mentioned binary TCOs based on In_2O_3 , SnO_2 and ZnO, ternary compounds such as Zn_2SnO_4 , ZnSnO_3 , $\text{Zn}_2\text{In}_2\text{O}_5$, $\text{Zn}_3\text{In}_2\text{O}_6$, $\text{In}_4\text{Sn}_3\text{O}_{12}$, and multi-component oxides including $(\text{ZnO})_{1-x}(\text{In}_2\text{O}_3)_x$, $(\text{In}_2\text{O}_3)_x(\text{SnO}_2)_{1-x}$, $(\text{ZnO})_{1-x}(\text{SnO}_2)_x$ are also the utilizable. Research in the early 80s focused on intrinsically doped ZnO thin films [101,102], but the electrical properties of these films were found to be unstable above 150 °C [103]. The stability issue was resolved by using extrinsically doped films. Further study presents a detail study of physical properties of as deposited and doped ZnO films by spray pyrolysis technique. From these one can conclude that excellent electrical properties of ZnO were possible to achieve which can be obtained at either elevated substrate temperatures or positioning the substrate perpendicular to the source.

1.2.4 Spray pyrolysis deposited ZnO thin films

A wide variety of chemical and physical deposition techniques have been applied in order to obtain high quality ZnO thin films, but the chemical spray is a safe, low-cost and simple technique. A lot of work on undoped ZnO thin films has been generated based through this technique [104]. Zinc oxide (ZnO) thin films deposited by chemical spray pyrolysis method usually show low resistivity, high transmittance in the visible spectrum, rough surface texture and chemical stability in the presence of hydrogen plasma [105-110]. It is worthy to note that some divergence exists among the different resistivities reported for the undoped ZnO films using dehydrated zinc acetate. S.E. Demian has reported ZnO films with resistivity magnitudes in the order of $2 \times 10^{-2} \Omega\text{-cm}$ [111], although it should be mentioned that this value is hard to obtain. The resistivity values more often reported lie in the range of 0-12 $\Omega\text{-cm}$ [112], 5-10 $\Omega\text{-cm}$ [113], 30-100 $\Omega\text{-cm}$ [107] and even 580 $\Omega\text{-cm}$ [106], in as-prepared films was used in all these cases. Unintentional doping was achieved with 2,4-zinc pentanedionate by the chemical spray technique [114]. The electrical, structural and

morphological properties of these films as a function of the substrate temperature were investigated. A resistivity of $2 \times 10^{-1} \Omega\text{-cm}$, a mobility of $11 \text{ cm}^2/\text{V s}$, a carrier concentration of $5 \times 10^{19} /\text{cm}^3$ and an average transmittance of 85% in the visible range were obtained for undoped ZnO films prepared at 500°C , with no post-annealing process [114]. Hichouet *et al.* reported the semiconducting metal oxide such as ZnO films were prepared by the spray pyrolysis technique on glass substrates and the cathodo-luminescence properties of these films were investigated with respect to deposition temperature and airflow rate [115]. The luminescent films had a polycrystalline hexagonal wurtzite-type structure. Cathodo-luminescence intensity was critically dependent on substrate temperature and spray rate. The best films had three emissions: nearultra-violet (UV) band gap peak at 382 nm, a blue-green emission at 520 nm and a red emission at 672 nm. These films were deposited at optimum conditions; $T_s=450^\circ\text{C}$ and $f = 5\text{ml}/\text{min}$ [115].

Hwang *et al.* showed in their short communication that transparent (>80% transmittance) ZnO thin films can be made by electrostatic spray deposition for 100 min at 300 and 400 °C on soda-lime-silica slide glass substrates with the X-ray diffraction analysis presence of poorly crystallized zinc oxide have formed. Along with they have observed band gap values of the ZnO films deposited at 300 and 400 °C are 3.28 and 3.24 eV, respectively [116]. Riadet *et al.* have reported the thin films of ZnO onto glass substrate at different substrate temperatures ranging from 180°C to 450 °C, have been prepared using a spray pyrolysis process [117]. The X-ray diffraction pattern showed that the films prepared at temperature greater than 300 °C were hexagonal wurtzitein structure with a preferential orientation along [0 0 2] direction. All electrical properties have been investigated for films at 400 °C. A relative permittivity of 9.8 is calculated from the capacitance measurements. Thermally generated electron concentration, $n = (2.8 - 6.7) \times 10^{10} \text{m}^{-3}$, and trapping factor, $\theta = (8.02 - 18.22) \times 10^{-12}$ have been evaluated from the analysis of current-voltage characteristics at room temperature assuming a plausible value of carrier mobility, $1.8 \text{m}^2/\text{V s}$ [117]. The structural, optical, chemical and electrical properties of thin films of ZnO obtained by spray pyrolysis over platinum (Pt) or silica substrates are determined at temperature ranges between 223 and 373 K by Ayouchiet *al.*[118]. The thin films of ZnO were pure with a preferred crystalline orientation of (0 0 2). Grain-boundary barriers were created by the band bending and the mobility of charge carriers is limited by the thermal field emission of electrons at the grain-boundary barriers [118].

Ayouchiet *al.* also reported that the structural, morphological, optical and electrical properties of ZnO thin films prepared by chemical spray pyrolysis from zinc acetate ($\text{Zn}(\text{CH}_3\text{COO})_2 \cdot 2\text{H}_2\text{O}$) aqueous solutions, on polished Si(1 0 0), and fused silica substrates for optical characterization, have been studied in terms of deposition time and substrate temperature [119]. The growth of the film presents three regimes depending on the substrate temperature. Paraguay *et al.* showed the zinc oxide thin films were prepared by spray pyrolytic decomposition of zinc acetate onto a glass substrate [120]. In their report Auger spectroscopy showed that the film stoichiometry is close to the ZnO phase with a little excess of oxygen. X-ray diffraction spectra show that the structure belongs to the hexagonal wurtzite crystal type, with a mean crystallite size in the range 20 ± 3 nm [120]. Mohammad *et al.* reported spray pyrolysis technique prepared highly conductive Al-doped ZnO films with high transparency [121]. The impurity had direct effect on the crystalline structure as indicated by shifting the X-ray diffraction peaks towards larger values of 2θ , where the atomic distances were reduced. Thin layers of $0.2 \mu\text{m}$ thick showed maximum conductivity of $0.3 (\Omega\text{-cm})^{-1}$, and transmittance of 70%, when prepared at substrate temperature of 430°C and 0.3% Al-doping [121].

The ZnO microrods were prepared by ultrasonic spray pyrolysis technique on glass substrates by Alveret *al.* In their paper, the X-ray diffraction patterns and scanning electron microscope images showed wurtzite-type ZnO rods within $1\text{--}3 \mu\text{m}$ diameters and 1 to $3 \mu\text{m}$ lengths. The XRD patterns exhibit hexagonal ZnO rods mainly grow along the [002] direction. The optical measurements reveal that films have maximum transmittance of about 80% and a direct band gap of 3.6 eV [122]. Sahayet *al.* reported that the ZnO thin films were prepared by spray pyrolytic decomposition of zinc acetate onto a glass substrate. The optical energy gaps for the films of different thicknesses are estimated to be in the range 2.98 – 3.09 eV. Electrical studies indicate that the films exhibit thermally activated electronic conduction and the activation energies are found to be dependent on the film thickness [123].

Tarwal and Patil have prepared super-hydrophobic and transparent ZnO thin films were deposited by spray pyrolysis technique (SPT) onto the glass substrates at 723K from an aqueous zinc acetate precursor solution [124]. The solution concentration was varied from 0.1 to 0.4M for which films were found to be polycrystalline, with preferential growth along *c*-axis. A slight improvement in the crystallite size and texture coefficient was observed as the concentration of the solution is increased. The SEM micrographs showed the uniform distribution of spherical grains of about 60–80nm grain size. The films were specular and

highly transparent with average transmittance of about 85%. The spectrum shows sharp absorption band edge at 381 nm, corresponding to optical gap of 3.25 eV [124].

Homogeneous and stoichiometric ZnO nanofibrous thin films were deposited onto cleaned glass substrate by a simple spray pyrolysis technique under atmospheric pressure using zinc acetate precursor at temperature 200 °C by Islam *et al.* [125]. The optical band gap of the ZnO thin films was found to be in the range 3.3 to 3.4 eV and the band-gap decreases with thickness of the film. Optical constants such as refractive index, extinction coefficient, real and imaginary parts of dielectric constants were evaluated from reflectance and absorbance spectra [125]. Ergin *et al.* have deposited ZnO film onto microscope glass substrates at 300 °C by ultrasonic spray pyrolysis technique to investigate its application potential in photovoltaic solar cells. Temperature dependent current measurements were performed by two-probe method to analyze electrical properties, and electrical conductivity at room temperature and activation energy values were calculated [126].

Hadjeris *et al.* in his report suggested a method to prepare ZnO films at different substrate temperatures and precursor molarity values. The films prepared at substrate temperatures above 400 °C appear better crystallized with (0 0 2) preferred orientation and exhibit higher visible transmittance (65–80%), higher electrical *n*-type semiconductor conductivity (10–50 ($\Omega\text{-cm}$)⁻¹), lower activation energy (<0.35 eV) and smaller Urbach energy (80 meV). These results indicate that such sprayed ZnO films are chemically purer and have many fewer defects and less disorder owing to an almost complete chemical decomposition of the precursor droplets [127]. Ashouret *et al.* have prepared thin films of ZnO have been prepared on glass substrates at different thicknesses by spray pyrolysis technique using 0.2 M aqueous solution of zinc acetate. The X-ray diffraction analysis of films reveals the polycrystalline in nature having hexagonal wurtzite-type crystal structure. The resistivity at room temperature is of the order 10⁻² $\Omega\text{-cm}$ and decreased as the temperature increased. The dependence of the refractive index, *n*, and extinction coefficient, *k*, on the wavelength for a sprayed film is also reported. Optical band gap (E_g) has been reported for the films. A shift from $E_g = 3.21$ eV to 3.31 eV has been observed for deposited films [128].

Joseph *et al.* proposed that undoped ZnO films have been prepared by chemical spray pyrolysis technique [129]. Using X-ray diffraction studies polycrystalline nature of the films with a hexagonal wurtzite type structure has been approved. Annealing in vacuum has reduced the resistivity of the films and the lowest value obtained was 3.15×10^{-3} $\Omega\text{-cm}$. The optical transmittance of the films in the visible region was found to be better than 95% in the

near-infrared and visible region [129]. Zhao *et. al.* have grown ZnO films by the ultrasonic spray pyrolysis method on ZnO seeding layer deposited on Si (100) by pulsed laser deposition [130]. The resultant film possessed a columnar microstructure perpendicular to the substrate and exhibits smooth, dense, and uniform morphology. The ZnO thin films, grown onto ZnO-seeded silicon exhibits higher hall mobility, lower resistivity and low photoluminescence intensity [130].

Goyal and Kachhwaha in their paper reported semiconducting ZnO whose band-gap can be tuned, which in turn finds various optical applications. Home-made spray pyrolysis technique is employed to prepare thin films. ZnO is II–VI group semiconductor material whose film was deposited on glass substrate using aqueous $ZnCl_2$ as a precursor. The XRD analysis showed polycrystalline nature of samples with pure phase formation. SEM analysis confirmed ZnO thin film contains oval shape and rod shaped particles. Resistance measurement as a function of temperature was done for ZnO thin films having semiconducting behavior were reported [131].

Alveret *al.* ZnO thin films were fabricated using zinc chloride and zinc acetate precursors by the spray pyrolysis technique on FTO coated glass substrates. The ZnO films were grown in different deposition temperatures range from 400 to 550 °C. The XRD patterns of the films deposited using chloride precursor indicate that (101) is dominant at low temperatures, while those deposited using acetate precursor show that (101) is dominant at high temperatures. Optical measurements show that ZnO films can be influenced by the substrate temperatures and different types of precursor solutions [132].

Prasada Rao *et al.* have also represented the effect of variation of substrate temperature on ZnO thin films deposited by spray pyrolysis technique onto glass substrates. The X-ray diffraction results showed the random growth orientation of the crystallites and the presence of the wurtzite phase of ZnO. The X-ray photoelectron spectroscopy (XPS) measurements reveal the presence of Zn^{2+} and chemisorbed oxygen in ZnO thin films. With AFM polycrystalline morphology and ~85% optical transmittance of ZnO thin film is obtained. Electrical resistivity was decrease; while the carrier concentration was increased with substrate temperature [133]. Rao *et al.* also reported that ZnO thin films onto various substrate temperatures by spray pyrolysis method. The evolution of strain and stress effects in ZnO thin films on glass substrate has been studied using X-ray diffraction. The films deposited at low substrate temperature have large compressive stress of 1.77 GPa, which relaxed to 1.47 GPa as the substrate temperature increased to 450 °C. All films exhibit a transmittance of about

85% in the visible region. It was found that the compressive stress in the films causes a decrease in the optical band gap [134].

Polymer-modified spray pyrolysis method used to deposit ZnO films onto alumina foil substrates by of zinc nitrate and zinc acetate solutions by Stambolova *et al.* [135]. The dependence of the concentration of added ethylcellulose and the type of zinc precursor on both the photocatalytic properties and films morphologies was investigated. The addition of ethylcellulose as a modifier in the spray solution led to the formation of a porous structure with crystallites sizes about 15 nm, when zinc acetate was used as precursor. These films show better photocatalytic activity for degradation of Malachite Green (MG) dye than the films obtained from zinc nitrate modified solution. The zinc nitrate films exhibit weaker activity for degradation of MG regardless of their smaller crystallite size (8–12 nm) [135].

Krunkset *al.* have applied chemical spray pyrolysis to grow ZnO nanorod arrays from zinc chloride solutions with pH=2 and 5 on glass/ITO substrate at 480 and 550 °C [136]. The charge carrier density in ZnO nanorods was determined from the C–V characteristics of ZnO/Hg Schottky barrier. Carrier densities $\sim 10^{15} \text{cm}^{-3}$ and slightly above 10^{16}cm^{-3} were obtained for ZnO deposited at 550 and 480 °C, respectively. According to PL studies, intense UV-emission was characteristic of ZnO independent of growth temperature, the concentration of oxygen vacancy related defects was lower in ZnO nanorods deposited at 550 °C [136]. The ZnO rod/In₂S₃/CuInS₂ type ETA-cells were prepared by Krunkset *al.* using inline chemical spray pyrolysis method. Effect of buffer layer thickness and ZnO nanorod length (500–1000nm) was studied by means of SEM, I–V dependencies and External Quantum Efficiency (EQE) spectra [137]. Conformal layer of In₂S₃, obtained by spray of solution with pH = 4.8, effectively protects ZnO nanorods from dissolution during the spray of acidic solutions [137].

Gledhill *et al.* have deposited ZnO by a spray pyrolysis process [138]. They have reported setup the aerosol of the precursor solution evaporates before landing on the substrate and hence is in principle an aerosol assisted chemical vapor deposition method. Without intentionally extrinsically doping the films and using only Zn(ac)₂ in the precursor solution, films with a relatively high carrier concentration ($\sim 8 \times 10^{18} \text{cm}^{-3}$) were obtained. The films exhibited poor carrier mobility due to the fine grain structure and undesired phases such as Zn(OH)₂ and Zn(ac)₂ in the subsequent film [138]. M. Bizarroin his paper reported that zinc oxide and aluminum doped zinc oxide films were deposited using the spray pyrolysis technique [139]. The aluminum incorporated improved greatly the photocatalytic efficiency

of ZnO films, reducing the degradation time of the MO dye from 4 to only 1.25 h (up to an 80% of degradation) following the next order of aluminum/zinc ratios added to the precursor solution: $0 < 0.05 < 0.10 < 0.25 < 0.50$. The photocatalytic activity improvement increased greatly for 0.10 and 0.25 Al/Znratios, but for higher concentrations this improvement reached to a saturation value [139].

Dedova *et al.* studied the formation of ZnO nanorods prepared by a spray pyrolysis technique on both as-received and etched ITO/glass substrates [140]. The morphologies of the ITO substrates, the ZnO nucleation mechanism and the development of ZnO nanorods on both types of ITO substrates were investigated by atomic force microscopy and scanning electron microscopy methods. As a result, well-shaped, elongated, strongly *c*-axis-oriented ZnO nanorods were obtained on the etched ITO/glass substrates [140]. Lehraki *et al.* with spray pyrolysis deposited ZnO thin films using different precursors. The starting solutions salts namely: zinc acetate, zinc chloride and zinc nitrate were used. The properties of these solutions and their influence upon ZnO films growth rate were investigated. A linear relationship between the solution dissociation energy and the growth rate activation energy was found. Both solution surface tension and dissociation enthalpy alter the microstructure of the formed film. Films deposited with zinc acetate were characterized by a smooth surface, dense network and high transparency, while films deposited with zinc chloride have a better crystallinity and low optical transmittance [141].

1.3 Properties of Zinc oxide (ZnO)

The ZnO is II–VI compound semiconductor showing structural, morphological, optical, electrical, piezoelectric and acoustic properties due to which it had various applications in field of electronics, spintronics and TCO. Zinc Oxide has some advantages over other alternate TCO materials such as In_2O_3 or SnO_2 due to its unique combination of interesting properties: non-toxicity, stability in a hydrogen plasma atmosphere good electrical, optical, piezoelectric behaviour, and moreover its low price.

1.3.1 Structural properties

ZnO exhibits wurtzite, zinc blende and rock salt structure. In addition to the wurtzite and zinc blende polymorphs, ZnO can be crystallized in the rock salt form at relatively high pressures about 10 GPa. ZnO has a near-perfect hexagonal wurtzite structure, as depicted in figure 1.2, consisting of Zn and O planes which are alternately stacked along the *c*-axis

direction. Therefore, as shown in figure 1.1, the crystal structures of ZnO are wurtzite (B4), zinc blende (B3), and rock-salt (B1) types. Under ambient conditions, the thermodynamically stable phase is wurtzite, while the zinc-blend ZnO structure is cubic; moreover, the rock-salt (NaCl) structure probably favors at relatively high pressure.

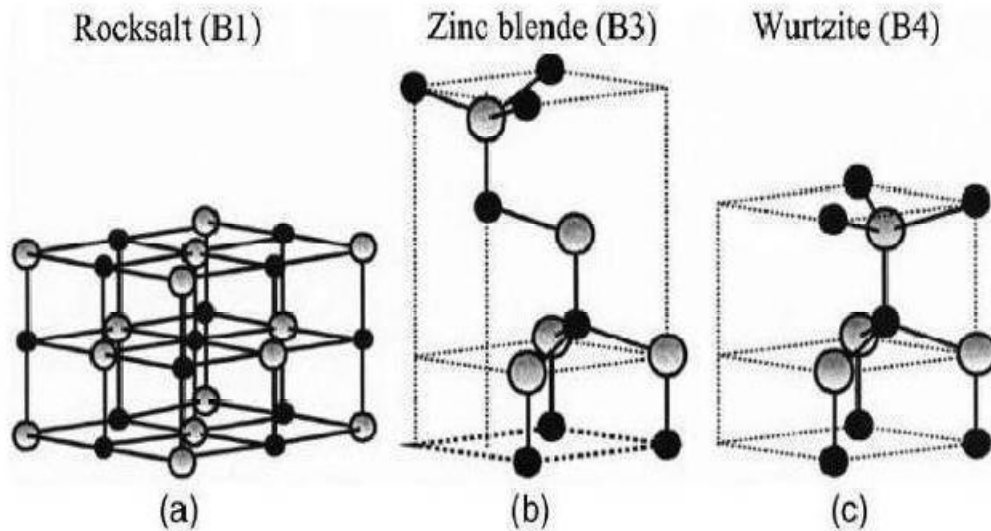


Figure 1.1: Stick and ball representation of ZnO crystal structures; (a) cubic rock-salt (B1), (b) cubic zinc blende (B3), and (c) hexagonal wurtzite (B4). The shaded gray and black spheres denote Zn and O atoms, respectively

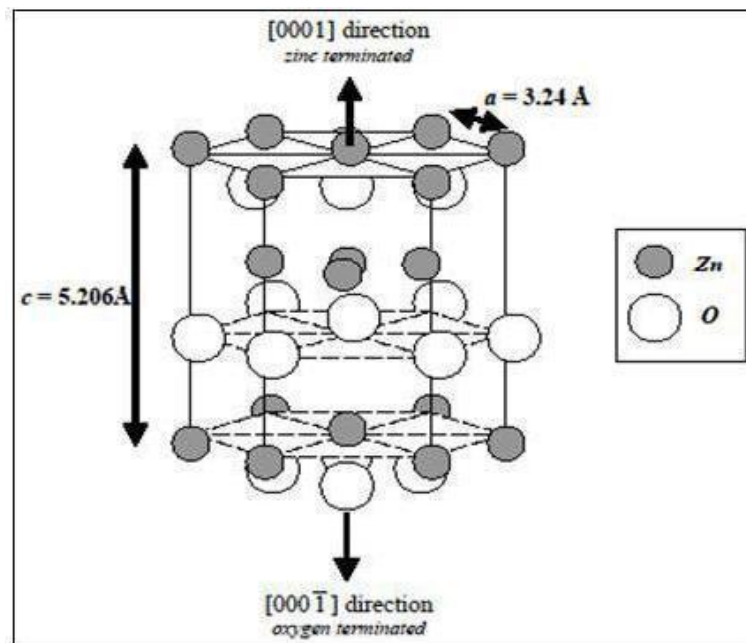


Figure 1.2: Hexagonal lattice structure of ZnO

Therefore, the structure of ZnO thin films deposited by SPD belongs to the wurtzite structure. The surface of ZnO may be Zn terminated ([0001]-oriented) or oxygen terminated ($\bar{1}\bar{1}\bar{2}$ -oriented). Each Zn atom is tetrahedral coordinated to four oxygen atoms. The ZnO is a near-perfect hexagonal lattice in the sense that the ratio between lattice parameters, c/a , is 1.602 as compared to the standard 1.633 value for a hexagonal lattice. The lattice parameters and the physical properties of ZnO are listed in Table 1.3.

Table 1.3: Physical properties of ZnO

Property	Value
Lattice parameters at 300K	
a_0	0.32495 nm
c_0	0.52069 nm
a_0/c_0	1.602
u	0.345
Density	5.606 g/cm ³
Stable Phase	Wurtzite
Melting point	1975 °C
Thermal conductivity	1-1.2
Linear expansion coefficient (/C)	$a_0=6.5 \times 10^{-6}$ $c_0= 3.0 \times 10^{-6}$
Static dielectric constant	8.656
Refractive index	2.008-2.029
Energy band gap	3.4 eV
Exciton binding energy	60 meV
Electron effective mass	0.24
Electron Hall mobility	200 cm ² /Vs
Hole effective mass	0.59
Hole Hall mobility	5-50 cm ² /Vs

1.3.2 Physical properties

ZnO can be grown on inexpensive substrate, such as glass, quartz at relatively low temperatures. It can be formed in different nanostructures, such as nanowires and nanorods,

nanobelts, nanoparticles having applications due to its large surface area-to-volume ratio [142]. The refractive index, energy band gap, hall mobility etc. these properties of ZnO make it an ideal candidate for a variety of devices ranging from sensors to ultra-violet laser diodes and nanotechnology-based devices such as displays due to fascinating properties such as thermal stability, resistance to high energy radiation, and varistor action.

1.3.3 Mechanical properties

As ZnO is II-VI compound semiconductor having elastic constant smaller than that GaN. It is relatively soft material with approximate hardness just 4.5. The high heat capacity and high heat conductivity, low values of thermal expansion and high melting points are some of the characteristics of ZnO. ZnO has been proposed to be a more promising UV emitting phosphor than GaN because of its larger exciton binding energy, discussed previously.

1.3.4 Optical properties

When light proceeds from one medium into another, several phenomena occur. Some of the light radiation may be transmitted through the medium, some will be absorbed, and some will be reflected at the interface on the surface. Moreover, the intensity I_0 of the beam incident on the surface of the thin films must equal the sum of the intensities of the transmitted, absorbed, and reflected beams, which can be written as $I_0 = I_T + I_A + I_R$. An alternate form of the above equation is $T + A + R = 1$, where T, A, R, respectively, are the transmittivity (I_T/I_0), absorptivity (I_A/I_0), and reflectivity (I_R/I_0). Thus, materials that are capable of transmitting light with relatively little absorption and reflection are transparent. The optical phenomenon occurs within solid materials, such as ZnO thin films; involve interactions between the electromagnetic radiation and atoms, ions and electrons. Of these interactions, electronic polarization and electron energy transitions are the most important. Nevertheless, absorption by electronic polarization is only explained for the light frequencies in the vicinity of the relaxation frequency of the constituent atoms [143]. Thus, for non-metallic materials like ZnO films at short wavelength (<400nm), absorption phenomena can be explained by the fundamental energy gap [144], which depends on the electron energy band structure of the materials; band structures for semiconductors like ZnO thin films are an important property.

As demonstrated in figure 1.3, absorption of a photon of light probably occurs by the promotion or excitation of an electron from the nearly filled valence band, across the band

gap, and into an empty state within the conduction band; a free electron in the conduction band and a hole in the valence band are created. Furthermore, the energy of excitation E is related to the absorbed photon frequency based on the electron transitions equation: $E=h\nu$. Thus, absorption phenomena can take place only if the photon energy is greater than the band gap E_g . This is represented as $h\nu > E_g$. Based on the above theory in which the absorption occurs by $h\nu > E_g$, we extend our discussion to metallic materials.

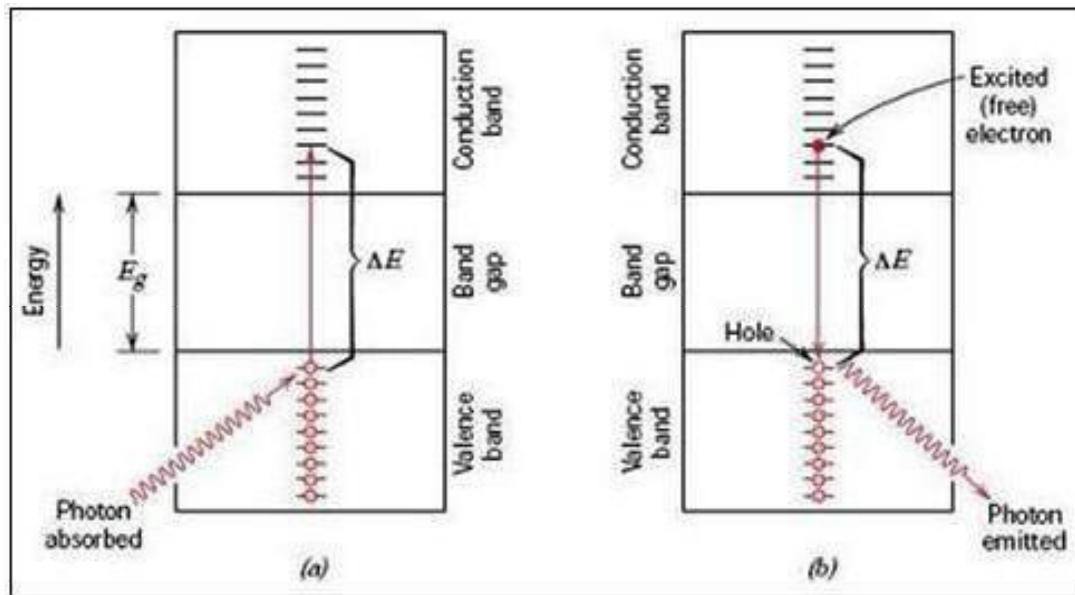


Figure 1.3: (a) Mechanism of photon absorption for non-metallic materials in which an electron is excited across the band gap, leaving behind a hole in the valence band. The energy of the photon absorbed is E , which is necessarily greater than the band gap energy E_g . (b) Emission of a photon of light by a direct electron transition across the band gap [144].

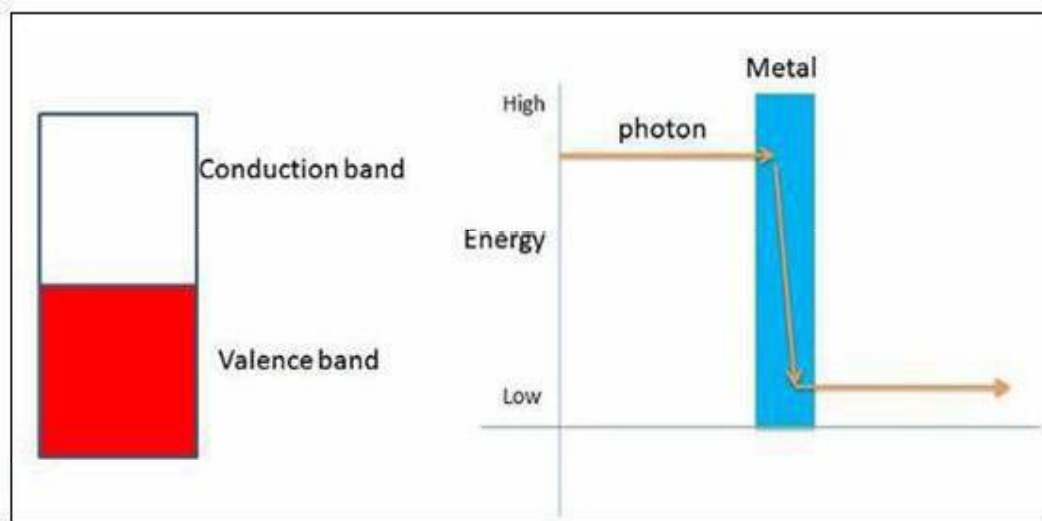


Figure 1.4: The relation between absorption and the energy band; metal.

As shown in figure 1.4, since metallic materials lack a band gap, every photon has enough energy to excite the electron into a higher energy unoccupied state. In contrast, for semiconductors like ZnO thin films, the absorption phenomenon occurs when the energy of the photon in some range of wavelength is greater than E_g while the transparency phenomenon occurs as that of photon under some range of wavelength is smaller than E_g shown in figure 1.5. Hence, that is the reason why the ZnO thin films are only transparent in the visible range; visible light lies within a very narrow region of the spectrum with wavelengths ranging between 400 nm to 700 nm [145].

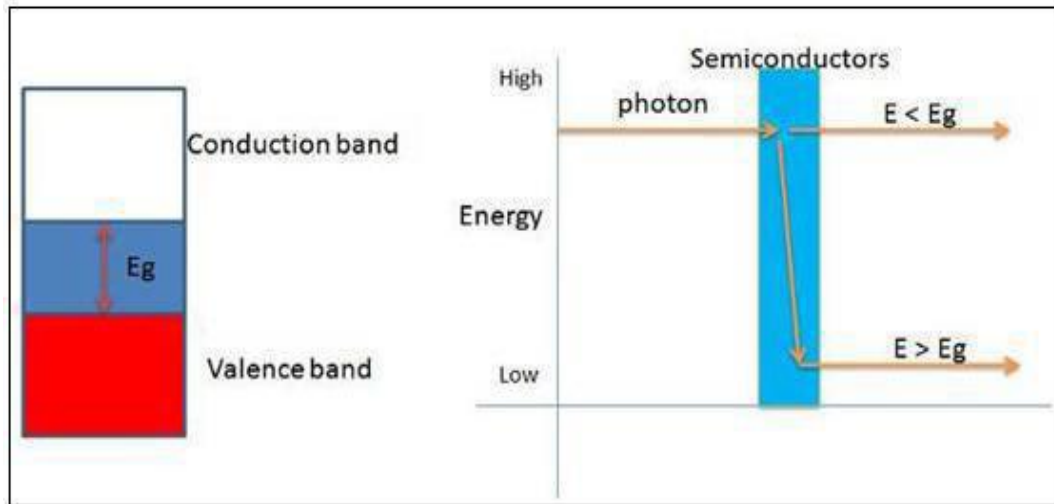


Figure 1.5: The relation between absorption and the energy band: semiconductors.

The transmittance and reflectance data can be used to calculate absorption coefficients of the films at different wavelengths. The absorption coefficient, α is given by the relation[144]:

$$\alpha = \frac{1}{t} \frac{(1-R)^2}{T} \quad (1.1)$$

where, 't' is the film thickness, T is the transmittance and R is the reflectance.

Additionally, the absorption coefficient (α) data also can be transferred to another equation relative to the band gap (E_g), which can be represented as the following:

$$\alpha h\nu = (h\nu - E_g)^{1/2} \quad (1.2)$$

where, $h\nu$ is the photon energy [146].

To design functional devices one need to understand these fundamental properties so that building blocks for nanoscale devices are feasible. Other physical properties of ZnO are discussed as below

1.3.5 Electrical properties

The electrical resistivity (ρ) of ZnO films is determined by the carrier concentration (n) and carrier mobility (μ), which is also presented as $\rho=1/(ne\mu)$ where 'e' is the electron charge. It is known that 'e' is a constant, so, for obtaining low resistivity, the carrier concentration and carrier mobility should be simultaneously maximized, and most research papers have suggested that the method of achieving maximum carrier concentration is by oxygen vacancies doping. Oxygen vacancies can be created by controlling the substrate temperature or ambient oxygen pressure. The literature [147] suggest, "If an oxygen vacancy is created in a perfect crystal, two electrons are created in the crystal and contributed as ionized donors." But, if there is too much oxygen vacancies created in the thin films, sub-oxides will form, causing the resistivity to rise."

In addition to the oxygen vacancies, doping also can change the electrical conduction of TCOs. As host cations are substituted by elements with a valence higher than that of the host, the extra electrons can become conduction electrons. To avoid the charge neutrality, substitution of a higher valence element creates extra electrons. It is well-known that pure ZnO films usually have a characteristic high resistivity due to their low carrier concentration. Therefore, in order to decrease resistivity, we can increase either the carrier concentration or the carrier mobility in zinc oxide thin films. The former is probably obtained by oxygen and/or zinc non-stoichiometry, or doping with an impurity.

However, Hu *et al.* [148] pronounced that non-stoichiometric films have excellent electrical and optical properties, but they become very unstable as the ambient temperature becomes higher. On the other hand, for obtaining stable low resistivity ZnO thin films, doped ZnO thin film is probably a good approach. In conclusion, the majority of research for achieving low resistivity ZnO thin films is focused on increasing the free carrier concentration in thin films through use of dopants and oxygen vacancies. But, Johnson *et al.* [149] in 1947 stated that increasing the carrier density via doping or oxygen vacancies is self-limiting because the increase of the number of free carriers decreases the mobility of carriers due to carrier-carrier scattering. Therefore, there is a trade-off relation between the carrier density and the carrier mobility for obtaining low resistivity.

1.4 Applications of ZnO

ZnO is best material with a wide range of applications. For material science applications such as materials and products including plastics, ceramics, glass, cement,

rubber, lubricants because of ZnO has high refractive index, high thermal conductivity, binding, antibacterial and UV-protection properties [150]. Also these properties make ZnO to be used in paints, ointments, adhesive, sealants, pigments, foods, batteries, ferrites, fire retardants, etc [151]. The ZnO nanorods result in a strong enhancement of an electric field therefore; they can be used as field emitters [152]. Commercial availability of ZnO makes them to be used as front contact for solar cells or of liquid crystal displays [153]. Transparent thin-film transistors and field-effect transistors also formed using ZnO. Some of the field-effect transistors even use ZnO nanorods as conducting channels [154]. The piezoelectricity in textile fibres coated in ZnO have been shown capable of fabricating "self-powered nanosystems" with everyday mechanical stress from wind or body movements [155].

Direct and wide band gap of ZnO ($\sim 3.37\text{eV}$) enables applications in optoelectronics including light-emitting diodes, laser diodes and photo detectors [156-160]. Large exciton binding energy of ZnO is promising for optical devices that are based on excitonic effects [161]. Piezoelectric ZnO films with uniform thickness and orientation have been grown on a variety of substrates using different deposition techniques, including sol-gel process; spray pyrolysis, chemical vapour deposition, molecular-beam epitaxy and sputtering. Sensors, transducers and actuator applications of ZnO are due to its large piezoelectric constants. [162-167].

n-type conductivity of ZnO and strong photoluminescence made it appropriate for applications in vacuum fluorescent displays, phosphor application and field emission displays [168]. Films of ZnO are used for detecting changes in electrical current passing through zinc oxide nanowires due to adsorption of gas molecules which has increased the sensitivity of the sensor device [169]. The conductivity of ZnO thin films is very sensitive to the exposure of the surface to various gases. ZnO thin films can be used as a sensor capable of detecting the freshness of foods and drinks, due to the high sensitivity to tri-methylamine present in the odor [170].

The non-linear optical response in ZnO thin films is attractive for integrated non-linear optical devices. ZnO films grown by laser deposition, reactive sputtering and spray pyrolysis show strong second-order non-linear response. Third-order non-linear response has recently been observed in ZnO nanocrystalline films [171]. During device fabrication high efficiency of removal of heat is possible for only materials having high thermal conductivity. This property makes ZnO useful as an additive in rubber in order to increase the thermal

conductivity of types [172]. It has been reported that ZnO thin films can be etched with acidic, alkaline as well as mixture solutions. This possibility of low-temperature chemical etching adds great flexibility in the processing, designing and integration of electronic and optoelectronic devices [173, 174].

1.5 Donor and acceptor levels in ZnO

1.5.1 Donor (*n*-type) levels

All nominally undoped ZnO films up to date are *n*-type in character. For a long time, the analysis of the temperature dependent Hall-effect measurements on high quality bulk ZnO grown by the vapor phase method has typically been shown to display two donors, a shallower one at 30-40 meV and a deeper one at 60-70 meV [175]. In a recent report though, the temperature dependent Hall-effect measurements on the same bulk ZnO has been shown to display three donors, with energy levels at about 30 meV, 44 meV and at around 60 meV [176]. In this section, the improvements in understanding the origin of the *n*-type conductivity of ZnO as revealed by various reports were discussed. The dominant donors in ZnO responsible for the observed *n*-type conductivity have for quite some time been attributed to the native defects, V_O [171] and Zn_i [177]. This assumption was the result of the abundance of *n*-type ZnO. The assumption was later challenged when Kohan *et al.* [178] in 2000 showed V_O and Zn_i were deep donors and also had high formation energies, thereby excluding them as possible dominant donors in ZnO. A later theoretical report by Zhang *et al.* [175] in 2001 showed that both V_O and Zn_i should indeed have donor transitions, but revealed that V_O is not a shallow donor but a deep donor and therefore could not be the dominant donor in ZnO. In the report by Zhang *et al.* [175] it was indeed shown that Zn_i is a shallow donor. But it is also reported however that both V_O and Zn_i have high formation energies. This suggests that they could not be the dominant donors in ZnO since they both cannot account for the high free carrier concentrations. In spite of all these findings about these native defects, some reports have adamantly attributed the *n*-type conductivity in their particular samples to either V_O or Zn_i .

The temperature dependent Hall-effect measurements proposed by Look *et al.* [177] on bulk ZnO measured 30 meV donor level (with a concentration of $6 \times 10^{15} \text{ cm}^{-3}$) is due to Zn_i or related complexes. Many researchers accepted the possibility of native defects not being the origin of the *n*-type conductivity in ZnO and therefore, diverted their attention to *n*-type impurity dopants as candidates in explaining the *n*-type conductivity in ZnO [175, 179].

The foremost one of these dopants that has perhaps been given a lot of attention by various researchers is hydrogen. This is the case because hydrogen is very abundant and can be easily incorporated in ZnO during the crystal growth process. Most importantly in ZnO, hydrogen occurs exclusively in the positive charge state, meaning that it always acts as a donor. Early experimental studies suggested that hydrogen in ZnO indeed acted as a donor [180-182]. Theyset *al.* [183] explained the increase in the *n*-type conductivity for their layers as a result of hydrogen introducing a donor level in ZnO. An alternative explanation is reported by Lavrov *et al.* [184] wherein introducing hydrogen into ZnO caused an increase in *n*-type conductivity. They attribute this increase in *n*-type conductivity to the passivation of the acceptors such as V_{Zn} and O_i . More about these acceptors is discussed in the next subsection [185].

Group III elements Al, B, Ga and In as substitutional elements for Zn and group-VII elements Cl and I as substitutional elements for O can be used as *n*-type dopants. Doping with Al, B, Ga, and In has been attempted by many groups, resulting in high-quality, highly conductive *n*-type ZnO films. The best candidate for this donor is thought to be Al:Zn, since it is known that Al is a contaminant of ZnO and that deliberate Al doping can produce very high free carrier concentrations [186]. The 60 meV donor has been measured in PLD ZnO layers grown on sapphire substrates as well [187].

1.5.2 Acceptor (*p*-type) levels

The nominally undoped, bulk ZnO, samples have also been shown by temperature dependent Hall effect measurements to be weakly compensated, with an acceptor concentration of only $2 \times 10^{15} \text{ cm}^{-3}$ [176]. Many potential acceptors in ZnO have been investigated in search for reproducible *p*-type ZnO. These acceptors include both the native defects and extrinsic *p*-type dopants. The most common intrinsic acceptors in ZnO are the V_{Zn} and O_i . The theoretical studies of Zhang *et al.* [175] revealed that these defects were shallow, meaning that they can supply holes even at room temperature. But the report also showed that these defects might bear high formation energies which mean that they can be easily compensated by the intrinsic donors such as V_O and Zn_i which have relatively lower formation energies. It is currently believed therefore, that ZnO cannot be doped *p*-type via native defects [188].

The *p*-type doping in ZnO may be possible by substituting either group-I elements (Li, Na, and K) for Zn sites acting as shallow acceptors and group-V elements (N, P, and As)

are found to act as deep acceptors on O sites. It was shown that group-I elements could be better *p*-type dopants than group-V elements in terms of shallowness of acceptor levels. However, group-I elements tend to occupy the interstitial sites, due to their small atomic radii, rather than substitutional sites, and therefore, they act as donors instead of acceptors. Moreover, significantly larger bond length for Na and K than ideal Zn–O bond length (1.93 Å) induces lattice strain, increasingly forming native defects such as vacancies which compensate the shallow dopants. Group V elements (N, P, As) except N, both P and As, have a larger bonds lengths. That's why they are likely to form antisites to avoid the lattice strain [189]. N appears to be good candidate for a shallow *p*-type dopant in ZnO with smallest ionization energy. This study is part of the ongoing research in the ZnO field because much of the ZnO-based technology is dependent on the control of doping in the material.

Without doubt, the most significant barrier to the widespread exploitation of ZnO related materials in electronic and photonic applications is the difficulty in carrier doping, particularly as it relates to achieving *p*-type material. With respect to *p*-type doping, ZnO displays significant resistance to the formation of shallow acceptor levels. The shallow level is shown in figure 1.6, in the band model of ZnO. The model consists of conduction band and valance band. The energy difference between them is the energy gap of ZnO, ~3.37 eV. The Fermi energy is the maximum energy level occupied by an electron at 0K.

Difficulty in achieving bipolar (*n*- and *p*-types) doping in a wide band gap material is common. These difficulties are; (i) the limited range of suitable shallow acceptors such as N [190] may be less soluble than the lowest achievable concentration of donors, (ii) the impurities that yield shallow acceptors on one site may act as donors when on another site or when at interstitials, and (iii) acceptors may have a natural tendency to pair with native defects or background impurities to form electrically inactive complexes [191, 192]. While most efforts to achieve *p*-type doping of ZnO have focused on nitrogen doping, a few studies have considered other group V elements for substitutional doping on the O site. Given the mismatch in ionic radii for P (2.12 Å), As (2.22 Å), N (1.32 Å) and Sb (2.45 Å) as compared to O (1.24 Å) [191], solubility of these elements in ZnO should be limited. The first *p*-type ZnO was reported in 1992, with many follow ups from 1997 onward [193]. There are some preliminary reports of phosphorus (P) [194], As [195], N [196, 197] (from NH₃, N₂ and N₂O etc.) doping and N-Al [198], N-Ga [199, 200] and N-In [201] co-doping *p*-type ZnO.

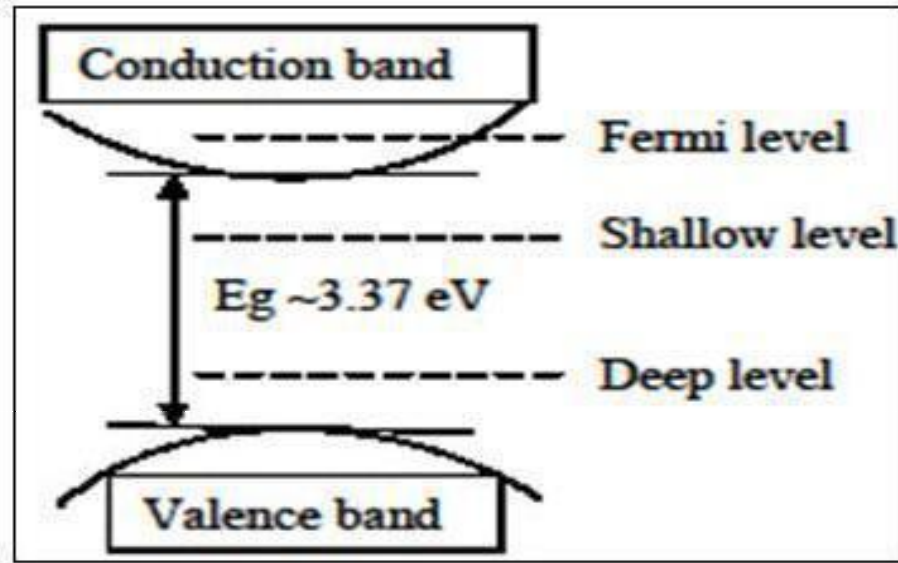


Figure 1.6: The band model for ZnO.

There are different growth techniques including chemical vapour deposition [194], pulsed laser deposition [160], molecular beam epitaxy [198], sputtering [196] and metalorganic chemical vapour deposition [202-204] etc., have been used for the successful growth of *p*-type ZnO. Many of them suffer from problems of instability and reproducibility. Dr. Look commented that “the future of ZnO light emitters depends on either producing low resistivity *p*-type ZnO, or in mating *n*-type ZnO with a *p*-type hole injector” [189].

1.6 Organization of the thesis

Based on literature and available studies in present work it is planned to synthesize transparent and conducting ZnO films onto glass substrate. At the first site details about a literature review of ZnO deposition by SPD method and implication of various characterization techniques employed are highlighted. Operation mechanisms are proposed in depth. The effects of air flow rate, precursor concentration, volume of precursor and substrate temperature variation with their physical and chemical properties on the ZnO thin films are investigated from the structure, morphology, optical and electrical properties points of view.

Effect of B doping on above properties is taken into consideration in next section which further extended for N doping too. In juxtra-pose, codoping of these metals is also carried out. Change in surface roughness, conductivity, transparency along with said properties are studied. The effect of the dopant concentration and substrate temperature on the conductivity and optical properties of the ZnO thin films is also discussed. The structural,

electrical and chemical compositional analysis also investigated. The main findings of the present work along with future plans are summarized at the end.

References:

- 1] D. Horwat, M. Jullien, F. Capon, J. F Pierson, J. Andersson, J. L Endrino, J. Phys. D: Appl. Phys. 43 (2010) 132003
- 2] D. J. Goyal, C. Agashe, M. G. Takawale, B. R. Marathe, V. G. Bhide, J. Mater. Sci. 27 (1992) 4705
- 3] K. Iwata, H. Tambo, A. Yamada, P. Fons, K. Matsubara, K. Sakurai, S. Ishizuka, S. Niki, Appl. Surf. Sci. 244 (2005) 504
- 4] M. T. Mohammad, A. A. Hashim, M. H. AlMaamory, Mater. Chem. Phys. 99 (2006) 382
- 5] R. Vinodkumar, K. J. Lethy, D. Beena, A. P. Detty, I. Navas, U. V. Nayar, V. P. Mahadevan Pillai, V. Ganesan, V. R. Reddy, Sol. Energy Mater. Sol. Cell. 94 (2010) 68
- 6] B. L. Zhu, X. Z. Zhao, F. H. Su, G. H. Li, X. G. Wu, J. Wua, R. Wu, Vacuum 84 (2010) 1280
- 7] Y. Wang, X. Li, N Wang, X. Quan, Y. Chen, Separation Purification Tech. 62 (2008) 727
- 8] S. L. Wang, X. Jia, P. Jiang, H. Fang, W. H. Tang, J. Alloy. Comp. 502 (2010) 118
- 9] Y. J. Chen, Y. Y. Shih, C. H. Ho, J. H. Du, Y. P. Fu, Cer. Int. 36 (2010) 69
- 10] X. Jiang, Y. Liu, Y. Gao, X. Zhang, L. Shi, Particuology 8 (2010) 383
- 11] J. Karamdel, C. F. Dee, B. Y. Majlis, Appl. Surf. Sci. 256 (2010) 6164
- 12] A. Goyal, S. Kachhwaha, Mater. Lett. 68 (2012) 354
- 13] M. Breedon, M. B. Rahmani, S. H. Keshmiri, W. Wlodarski, K. KalantarZadeh, Mater. Lett. 64 (2010) 291
- 14] P. Thilakan, D. M. Radheep, K Saravanakumar, G. Sasikala, Semicond. Sci. Technol. 24 (2009) 085020
- 15] M. H. Valdés, M. Berruet, A. Goossens, M. Vázquez, Surf. Coat. Technol. 204 (2010) 3995
- 16] C. G. Granqvist, Sol. Energy Mater. Sol. Cell. 91 (2007) 1529
- 17] T. Minami, Semicond. Sci. Technol. 20 (2005) S35
- 18] G. J. Exarhos, X. D. Zhou, Thin Solid Film 515 (2007) 7025
- 19] K. Badeker, Ann. Phys. (Berlin) 22 (4) (1907) 749
- 20] L. Holland, G. Siddall, Vacuum 3 (1953) 375
- 21] R. Groth, E. Kauer, Philips Tech. Rev. 26 (1965) 105

-
- 22] A. Walsh, J. L. D. Silva, S. H. Wei, C. Körber, A. Klein, L. F. Piper, A. DeMasi, K. E. Smith, G. Panaccione, P. Torelli, D. J. Payne, A. Bourlange, R. G. Egdell, *Phys. Rev. Lett.* 100 (2008) 167402
- 23] P. D. C. King, T. D. Veal, F. Fuchs, Ch. Y. Wang, D. J. Payne, A. Bourlange, H. Zhang, G. R. Bell, V. Cimalla, O. Ambacher, R. G. Egdell, F. Bechstedt, C. F. McConville, *Phys. Rev. B* 79 (2009) 205211
- 24] T. Minami, *Thin Solid Film* 516 (2008) 5822
- 25] H. Hara, T. Shiro, T. Yatabe, *Japn. J. Appl. Phys.* 43 (2004) 745
- 26] M. Batzill, U. Diebold, *Prog. Surf. Sci.* 79 (2005) 47
- 27] D. S. D. Amma, V. K. Vaidyan, P. K. Manoj, *Mater. Chem. Phys.* 93 (2005) 194
- 28] J. W. Bae, S. W. Lee, G. Y. Yeom, *Electrochem. Soc.* 154 (2007) D34
- 29] S. W. Lee, Y. W. Kim, H. D. Chen, *Appl. Phys. Lett.* 78 (2001) 350
- 30] S. R. Dhage, V. Ravi, *Appl. Phys. Lett.* 83 (2003) 4539
- 31] Y. Wang, T. Brezesinski, M. Antonietti, B. Smarsly, *ACS Nano* 3 (2009) 1373
- 32] T. Kawashima, T. Ezure, K. Okada, H. Matsui, K. Goto, N. Tanabe, *J. Photochem. Photobiol. A: Chemical* 164 (2004) 199
- 33] M. Oshima, Y. Takemoto, K. Yoshino, *Phys. Status Solidi C* 6 (2009) 1124
- 34] A. G. Macedo, C. E. Cava, C. D. Canestraro, L. Contini, L. S. Roman, *Microsc. Microanal.* 11 (2005) 118
- 35] W. J. Lee, D. Y. Lee, J. S. Song, B. K. Min, *Met. Mater. Int.* 11 (6) (2005) 465
- 36] P. Gerhardinger, D. Strickler, *Engg. Mater.* 380 (2008) 169
- 37] H. J. Ko, Y. F. Chen, S. K. Hong, H. Wensch, T. Yao, D. C. Look, *Appl. Phys. Lett.* 77 (2000) 3761
- 38] V. Bhosle, A. Tiwari, J. Narayan, *Appl. Phys. Lett.* 88 (2006) 032106
- 39] B. K. Meyer, H. Alves, D. M. Hofmann, W. Kriegseis, D. Forster, F. Bertram, J. Christen, A. Hoffmann, M. Straburg, M. Dworzak, U. Haboek, A. V. Rodina, *Phys. Status Solidi.* 241 (2004) 231
- 40] H. Agura, H. Suzuki, T. Matsushita, T. Aoki, M. Okuda, *Thin Solid Film* 445 (2003) 263
- 41] S. M. Park, T. Ikegami, K. Ebihara, *Thin Solid Film* 513 (2006) 90
- 42] H. Ohta, M. Orita, M. Hirano, H. Tanji, H. Kawazoe, H. Hosono, *Appl. Phys. Lett.* 76 (2000) 2740
- 43] B. Z. Dong, G. J. Fang, J. F. Wang, W. J. Guan, X. Z. Zhao, *J. Appl. Phys.* 101 (2007) 033713

- 44] S. Shirakata, T. Sakemi, K. Awai, T. Yamamoto, *Superlattices Microstruct.* 39 (2006) 218
- 45] H. Y. Liu, V. Avrutin, N. Izyumskaya, M. A. Reshchikov, U. Ozgür, H. Morkoç, *Phys. Status Solidi RRL* 4 (3–4) (2010) 70
- 46] J. J. Berry, D. S. Ginley, P. E. Burrows, *Appl. Phys. Lett.* 92 (2008) 193304
- 47] A. Suzuki, T. Matsushita, T. Aoki, A. Mori, M. Okuda, *Thin Solid Film* 411 (2002) 23
- 48] Y. Sawada, C. Kobayashi, S. Seki, H. Funakubo, *Thin Solid Film* 409 (2002) 46
- 49] O. Tuna, Y. Selamet, G. Aygun, L. Ozyuzer, *J. Phys. D: Appl. Phys.* 43 (2010) 055402
- 50] A. I. Martínez, L. Huerta, J. M. O-Rueda de León, A. Acosta, O. Malik, M. Aguilar, *J. Phys. D: Appl. Phys.* 39 (2006) 5091
- 51] A. V. Moholkar, S. M. Pawar, K. Y. Rajpure, C. H. Bhosale, J. H. Kim, *Appl. Surf. Sci.* 255 (2009) 9358
- 52] E. Elangovan, K. Ramamurthi, *Appl. Surf. Sci.* 249 (2005) 183
- 53] J. W. Bae, S. W. Lee, G. Y. Yeom, *Electrochem. Soc.* 154 (2007) D34
- 54] T. Ohgaki, Y. Kawamura, T. Kuroda, N. Ohashi, Y. Adachi, T. Tsurumi, F. Minami, H. Haneda, *Key Engg. Mater.* 248 (2003) 91
- 55] J. G. Lu, S. Fujita, *J. Appl. Phys.* 101 (2007) 083705
- 56] H. Wang, M. Xu, J. Xu, M. Ren, L. Yang, *J. Mater. Sci. Mater. Electronics* 21 (2010) 589
- 57] F. Ruske, M. Roczen, K. Lee, M. Wimmer, S. Gall, J. Hüpkes, D. Hrunski, B. Rech, *J. Appl. Phys.* 107 (2010) 013708
- 58] T. Minami, H. Nanto, S. Takata, *Japn. J. Appl. Phys.* 23 (1984) L280
- 59] T. Minami, K. Oohashi, S. Takata, T. Mouri, N. Ogawa, *Thin Solid Film* 193 (1990) 721
- 60] S. H. Jeong, J. H. Boo, *Thin Solid Films* 447 (2004) 105
- 61] A. Suzuki, T. Matsushita, N. Wada, Y. Sakamoto, M. Okuda, *Japn. J. Appl. Phys.* 35 (1996) L56
- 62] H. Agura, H. Suzuki, T. Matsushita, T. Aoki, M. Okuda, *Thin Solid Film* 445 (2003) 263
- 63] B. Z. Dong, H. Hu, G. J. Fang, X. Z. Zhao, D. Y. Zheng, Y. P. Sun, *J. Appl. Phys.* 103 (2008) 073711
- 64] K. Nakahara, K. Tamura, M. Sakai, D. Nakagawa, N. Ito, M. Sonobe, H. Takasubel, H. Tampo, P. Fons, K. Matsubara, K. Iwata, A. Yamada, S. Niki, *Japn. J. Appl. Phys.* 43 (2004) L180
- 65] K. Tamura, K. Nakahara, M. Sakai, D. Nakagawa, N. Ito, M. Sonobe, H. Takasu, H. Tampo, P. Fons, K. Matsubara, K. Iwata, A. Yamada, S. Niki, *Phys. Status Solidi* 201 (2004) 2704

- 66] M. Law, L. E. Greene, J. C. Johnson, R. Saykally, P. Yang, *Nature Mater.* 4 (2005) 455
- 67] H.Y. Liu, X. Li, X. Ni, V. Avrutin, N. Izyumskaya, Ü. Özgür, H. Morkoç, *Proc. SPIE* 7602 (2010) 76020I
- 68] B. M. Ataev, A. M. Bagamadova, V. V. Mamedov, *J. Cryst. Growth* 1222 (1999) 198
- 69] J. K. Sheu, M. L. Lee, Y. S. Lu, K. W. Shu, *IEEE J. Quantum Electron.* 44 (2008) 1211
- 70] S. M. Park, T. Ikegami, K. Ebihara, *Thin Solid Film* 513 (2006) 90
- 71] L. Manna, D. J. Milliron, A. Meisel, E. C. Scher. A. PAUL Alivisatos, *Nature Mater.* 2 (2003) 382
- 72] J. M. Mochel, Patent# 2, USA (1947) 564
- 73] H. A. McMaster, Patent# 2, USA (1947) 429
- 74] W. O. Lytle, Patent# 2, USA (1951) 566
- 75] J. M. Mochel, Patent# 2, USA (1951) 564
- 76] L. Holland and G. Siddall, *Vacuum* III (1955)
- 77] H. F. Dates and J. K. Davis, Patent# 3, USA (1967) 331
- 78] A. J. Nozik, Patent# 3, USA (1974) 811
- 79] A. J. Nokik, G. Haacke, Patent# 3, USA (1976) 957
- 80] R. G. Gordon, Patent# 4, USA (1979) 146
- 81] S. R. Kurtz, R. G. Gordon, *Thin Solid Film* 139 (1986) 277
- 82] S. Major, A. Banerjee, and K. L. Chopra, *Thin Solid Film* 122 (1984) 31
- 83] T. Minami, H. Nanto, S. Takata, *Jpn. J. Appl. Phys. Lett.* 23 (1984) L280
- 84] S. N. Qiu, C. X. Qiu, I. Shih, *Sol. Energy Mater.* 15 (1987) 261
- 85] P. S. Vijayakumar, K. A. Blaker, R. D. Weiting, B. Wong, A. T. Halani, C. Park, Patent# 4, USA (1988) 751
- 86] B. H. Choi, H. B. Im, J. S. Song, K. H. Yoon, *Thin Solid Film* 193 (1990) 712
- 87] J. Hu, R. G. Gordon, *Sol. Cell.* 30 (1990) 437
- 88] J. Hu, R. G. Gordon, *J. Appl. Phys.* 71 (2) (1992) 880
- 89] J. Hu, R. G. Glordon, *J. Appl. Phys.* 72 (11) (1992) 5381
- 90] J. Hu, R. G. Gordon, "Proceedings of Fall Materials Research Society: Microcrystalline Semiconductors: Materials Science and Devices Symposium", Boston, MA, 1993
- 91] H. Enoki, T. Nakayama, J. Echigoya, *Physica Status Solidi A* 129 (1) (1992) 181
- 92] T. Minami, H. Sonohara, S. Takata, and H. Sato, *Jpn. J. Appl. Phys.* 433 (1994) L1693
- 93] S. Zhao, W. Liu, L. Yang, K. Zhao, H. Liu, N. Zhou, A. Wang, Y. Zhou, Q. Zhou, Y. Shi, *J. Phys. D: Appl. Phys.* 42 (2009) 185101

- 94] B. Kotlyarchuk, V. Savchuk, M. Oszwaldowski, *Cryst. Res. Technol.* 40 (12) (2005) 1118
- 95] K. Yoshino, S. Oyama, M. Kato, M. Oshima, M. Yoneta, T. Ikari, *J. Phys. Conf. Ser.* 100 (2008) 082019
- 96] Q. Yu, W. Fu, C. Yu, H. Yang, R. Wei, Y. Sui, S. Liu, Z. Liu, M. Li, G. Wang, C. Shao, Y. Liu, G. Zou, *J. Phys. D: Appl. Phys.* 40 (2007) 5592
- 97] S. Ilican, Y. Caglar, M. Caglar, F. Yakuphanoglu, *Appl. Surf. Sci.* 255 (2008) 2353
- 98] K. K. Kim, S. D. Lee, H. Kim, J. C. Park, S. N. Lee, Y. Park, S. J. Park, S. W. Kim, *Appl. Phys. Lett.* 94 (2009) 071118
- 98] J. Zhong, H. Chen, G. Saraf, Y. Lu, C.K. Choi, J.J. Song, D.M. Mackie, H. Shen, *Appl. Phys. Lett.* 90 (2007) 203515
- 99] J. H. Lee, C. Y. Chou, Z. Bi, C. F. Tsai, H. Wang, *Nanotechnol.* 20 (2009) 395704
- 100] F. J. Pern, R. Noufi, X. Li, C. DeHart, B. To, Presented at the 33rd IEEE Photovoltaic Specialists Conference San Diego, California, May 11–16, 2008
- 101] S. Maniv, C. J. Miner, W. D. Westwood, *J. Vacuum Sci. Technol. A* 1 (1983) 1370
- 102] T. Minami, H. Nanto, S. Takata, *Appl. Phys. Lett.* 40 (1982) 961
- 103] T. Minami, H. Nanto, S. Shooji, S. Takata, *Thin Solid Film* 111 (2) (1984) 167
- 104] K. L. Chopra, S. Major, D. K. Pandya, *Thin Solid Film* 102 (1983) 1
- 105] M. Krunk, E. Mellikov, *Thin Solid Film* 270 (1995) 33
- 106] P. Nunes, B. Fernandes, E. Fortunato, P. Vilarinho, R. Martins, *Thin Solid Film* 337 (1999) 176
- 107] A. Ortiz, A. Sanchez, C. Falcony, M. H. Farias, G. A. Hirata, L. Cota-Araiza, *J. Non-Crystalline Solid* 103 (1988) 9
- 108] M. de la L. Olvera, A. Maldonado, R. Asomoza, M. Konagai, M. Asomoza, *Thin Solid Film* 229 (1993) 196
- 109] G. Haacke, *J. Appl. Phys.* 47 (1976) 4086
- 110] S. Major, A. Banerjee, K. L. Chopra, *Thin Solid Film* 41 (1984) 154
- 111] S. E. Demian, *J. Mater. Sci. Mater. Electronic* 5 (1994) 360
- 112] M. N. Islam, M. O. Hakim, H. Rahman, *J. Mater. Sci.* 22 (1987) 1379
- 113] C. Eberspacher, A. L. Fahrenbruch, R. H. Bube, *Thin Solid Film* 136 (1986) 1
- 114] M. de la L. Olvera, A. Maldonado, R. Asomoza, S. Tirado-Guerra, *Thin Solid Film* 411 (2002) 198
- 115] A. E. Hichou, M. Addouc, J. Ebothe, M. Troyon, *J. Luminescence* 113 (2005) 183

- 116] K. S. Hwang, J. H. Jeong, Y. S. Jeon, K. O. Jeon, B. H. Kim, *Ceramics International* 33 (2007) 505
- 117] A. S. Riad, S. A. Mahmoud, A. A. Ibrahim, *Physica B* 296 (2001) 319
- 118] R. Ayouchi, D. Leinen, F. Martina, M. Gabas, E. Dalchiale, J. R. Ramos-Barrado, *Thin Solid Film* 426 (2003) 68
- 119] R. Ayouchi, F. Martin, D. Leinen, J. R. Ramos-Barrado, *J. Crystal Growth* 247 (2003) 497
- 120] F. D. Paraguay, W. L. Estrada, D. R. N. Acosta, E. Andradeb., M. Miki-Yoshida, *Thin Solid Film* 350 (1999) 192
- 121] M. T. Mohammad, A. A. Hashim, M. H. Al-Maamory, *Mater. Chem. Phys.* 99 (2006) 382
- 122] U. Alver, T. Kılınç, E. Bacaksız, T. Küçükömeroğlu, S. Nezir, İ.H. Mutlu, F. Aslan, *Thin Solid Film* 515 (2007) 3448
- 123] P. P. Sahay, S. Tewari, R. K. Nath, *Cryst. Res. Technol.* 42 (2007) 723
- 124] N. L. Tarwal, P. S. Patil *Appl. Surf. Sci.* 256 (2010) 7451
- 125] M. R. Islam, J. Podder, *Cryst. Res. Technol.* 44 (2009) 286
- 126] B. Ergin, E. Ketenci, F. Atay, *International J. Hydrogen Energy* 34 (2009) 5249
- 127] L. Hadjeris, L. Herissi, M. B. Assouar, T. Easwarakhanthan, J. Bougdira, N. Attaf, M. S. Aida, *Semicond. Sci. Technol.* 24 (2009) 035006
- 128] A. Ashour, M. A. Kaid, N. Z. El-Sayed, A. A. Ibrahim, *Appl. Surf. Sci.* 252 (2006) 7844
- 129] B. Joseph, K. G. Gopchandran, P. V. Thomas, Peter Koshy, V. K. Vaidyan, *Mater. Chem. Phys.* 58 (1999) 71
- 130] J. L. Zhao, X. M. Li, S. Zhang, C. Y. X. D. Gao, W. D. Yu, *J. Mater. Res.* 21 (2006) 2185
- 131] A. Goyal, S. Kachhwaha, *Mater.Lett.* 68 (2012) 354
- 132] U. Alver, A. Kudret, S. Tekerek, *J. Phys. Chem. Solid* 72 (2011) 701
- 133] T. P. Rao, M. C. S. Kumar, A. Safarulla, V. Ganesan, S. R. Barman, C. Sanjeeviraja, *Physica B.* 405 (2010) 2226
- 134] T. P. Rao, M. C. S. Kumar, S. A. Angayarkanni, M. Ashok, *J.Alloy.Compound.* 485 (2009) 413
- 135] I. Stambolova, V. Blaskov, M. Shipochka, S. Vassilev, C. Dushkin, Y. Dimitriev, *Mater. Chem. Phys.* 121 (2010) 447

- 136] M. Krunk, T. Dedova, E. Karber, V. Mikli, I. OjaAcik, M. Grossberg, A. Mere, *Physica B*. 404 (2009) 4422
- 137] M. Krunk, E. Karber, A. Katerski, K. Otto, I. OjaAcik, T. Dedov, A. Mere *Sol. Energy Mater. Sol. Cell*. 94 (2010) 1191
- 138] S. Gledhill, A. Grimm, D. Greiner, W. Bohne, M. Lux-Steiner, C. H. Fischer, *Thin Solid Film* 519 (2011) 4293
- 139] M. Bizarro, *Appl. Catalysis B: Environmental* 97 (2010) 198
- 140] T. Dedova, I. OjaAcik, M. Krunk, V. Mikli, O. Volobujeva, A. Mere, *Thin Solid Film* 520 (2012) 4650
- 141] N. Lehraki, M. S. Aida, S. Abed, N. Attaf, A. Attaf, M. Poulain, *Curr. Appl. Phys.* 12 (2012) 1283
- 142] K. S. Leschkies, T. J. Beatty, M. S. Kang, D. J. Norris, E. S. Aydil, *ACS Nano* 3 (2009) 3638
- 143] W. D. Callister, *J. Fundamental. Mater. Sci. Engg.* Fifth edition ed. John Wiley & Sons, Inc, New York 2000
- 144] K. L. Chopra, S. Major, D. K. Pandya, *Thin Solid Film* 102 (1983) 1
- 145] V. Srikant, D. R. Clarke, *J. Appl. Phys.* 83(1998) 5447
- 146] J. Tauc, R. Grigorovici, A. Vancu, *Physica Status Solidi* 15 (1966) 627
- 147] B. L. Zhu, X. Z. Zhao, F. H. Su, G. H. Li, X. G. Wu, J. Wu, R. Wu, *Vacuum* 84 (2010) 1280
- 148] J. Hu, R. G. Gordon, *J. Appl. Phys.* 71 (1992) 880
- 149] V. A. Johnson, K. Lark-Horovitz, *Phys. Rev.* 92 (1953) 226
- 150] Y. Yoshino, T. Makino, Y. Katayama, *Vacuum*, 59 (2000) 538
- 151] W. C. Shin, M. S. Wu, *J. Cryst. Growth* 137 (1994) 319
- 152] R. Das, S. Ray, *J. Phys. D: Appl. Phys.* 36 (2003) 152
- 153] K. Ellmer, *J. Phys. D: Appl. Phys.* 33 (2000) R 17
- 154] Y. Zhang, G. Du, X. Yang, B. Zhao, Y. Ma, T. Yang, H. C. Ong, D. Liu, S. Yang, *Semicond. Sci. Technol.* 19 (204) 755
- 155] K. Govender, D. S. Boyle, P. O. Brien, D. Binks, D. West, D. Coleman, *Adv. Mater.* 14 (2002) 1221
- 156] D. C. Look, *Mater. Sci. Eng. B* 80 (2001) 383
- 157] U. Ozgur, Y. I. Alivov, C. Liu, A. Teke, M. A. Reshchikov, S. Dogan, V. Avrutin, S. J. Cho, H. Morkoc, *J. Appl. Phys.* 98 (2005) 041301

- 158]** C. W. Nahm, *Ceramics International* 36 (2010) 1109
- 159]** J. P. Kar, S. N. Das, J. H. Choi, T. I. Lee, J. M. Myoung, *Appl. Surf. Sci.* 256 (2010) 4995
- 160]** Y. Wang, C. Zhang, S. Bi, G. Luo, *Powder Technol.* 202 (2010) 130
- 161]** X. Zhang, H. Fan, J. Sun, Y. Zhao, *Thin Solid Film* 515 (2007) 8789
- 162]** M. N. Kamalasanan, S. Chandra, *Thin Solid Film* 288 (1996) 112
- 163]** F. D. Paraguay, W. L. Estrada, D.R.N. Acosta, E. Andrade, M. Miki-Yoshida, *Thin Solid Film* 350 (1999) 192
- 164]** H. Funakubo, N. Mizutani, M. Yonetsu, A. Saiki, K. Shinozaki, *J. Electroceram.* 4 (1999) S1
- 165]** K. Sakurai, M. Kanehiro, K. Nakahara, T. Tanabe, S. Fujita, *J. Cryst. Growth* 209 (2000) 522
- 166]** T. Yamamoto, T. Shiosaki, A. Kawabata *J. Appl. Phys.* 51 (1980) 113
- 167]** J. Molarius, J. Kaitila, T. Pensala, M. Ylimlammi, *J. Mater. Sci. Mater. Electron.* 14 (2003) 431
- 168]** X. D. Zhang, H. B. Fan, J. Sun, Y. Zhao, *Physica E* 39 (2007) 267
- 169]** D. S. Boyle, K. Govender, P. O. Brien, *Chem. Commn.* (2002) 3773
- 170]** H. Nanto, H. Sokooshi, T. Usuda, *Solid State Sensor Actuator* 24 (1998) 596
- 171]** M. C. Larciprete, *Appl. Phys. B Lasers Opt.* 82 (2006) 431
- 172]** D. I. Florescu, L. G. Mourokh, F. H. Pollak, D. C. Look, G. Cantwell, X. Li, *J. Appl. Phys.* 91 (2002) 890
- 173]** U. Ozgur, X. Gu, S. Chevtchenko, J. Spradlin, S-J. Cho, H. Morkoc, F. H. Pollak, H. Everitt, B. J. Nemeth, J. E. Nause, *J. Electr. Mater.* 35 (2006) 550
- 174]** K. Maeda, M. Sato, I. Niikura, T. Fukuda, *Semicond. Sci. Technol.* 20 (2005) S49
- 175]** S. B. Zhang, S. H. Wei, A. Zunger, *Phys. Rev. B* 63 (2001) 075205
- 176]** Z. Gao, Y. Gu, Y. Zhang, *J. Nanomater.* 32 (2010) 1
- 177]** D. C. Look, J. W. Hemsky, J.R. Sizelove, *Phys. Rev. Lett.* 82 (1999) 2552
- 178]** A. F. Kohan, G. Ceder, D. Morgan, C. G. Van de Walle, *Phys. Rev. B* 61 (2000) 15019
- 179]** D. C. Look, G. C. Farlow, P. Reunchan, S. Limpijumnong, S. B. Zhang, K. Nordlund, *Phys. Rev. Lett.*, 95 (2005) 225502
- 180]** E. Mollwo, *J. Phys. B* 138 (1954) 478
- 181]** D. G. Thomas, J. J. Lander, *J. Chem. Phys.* 25 (1956) 1136
- 182]** J. J. Lander, *J. Phys. Chem. Solids*, 3 (1957) 87

- 183]** B. Theys, V. Sallet, F. Jomard, A. Lusson, *J. Appl. Phys.*, 91 (2002) 3922
- 184]** E.V. Lavrov, F. Bornert, J. Weber, *Phys. Rev. B*, 71 (2005) 055205
- 185]** K. Ip, M. E. Overberg, Y. W. Heo, D. P. Norton, S. J. Pearton, C. E. Stutz, S. O. Kucheyev, C. Jagadish, J. S. Williams, B. Luo, F. Ren, D. C. Look, J. M. Zavada, *Sol. Stat. Electr.* 47 (2003) 2255
- 186]** D. C. Look, H. L. Mosbacker, Y. M. Strzhemechny, L. J. Brillson, *Superlattice Microstructure* 38 (2005) 406
- 187]** M. Grundmann, H. V. Wenckstern, R. Pickenhain, Th. Nobis, A. Rahm, M. Lorenz, *Superlattice Microstructure*.38 (2005) 317
- 188]** D. C. Look, C. Coskun, B. Claflin, G. C. Farlow, *Physica B*, 340-342 (2003) 32
- 189]** D. C. Look, *Semicond. Sci. Technol.* 20 (2005) S55
- 190]** X. D. Gao, X. M. Li, W. D. Yu, *Mater. Res. Bull.* 40 (2005) 1104
- 191]** N. Asakuma, H. Hirashima, H. Imai, T. Fukuki, A. Maruta, M. Toki, K. Awazu *J. Appl. Phys.* 92 (2002) 5707
- 192]** J. H. Lee, K. H Ko, B. O. Park, *J. Cryst. Growth* 247 (2003) 119
- 193]** H. Li, J. Wang, H. Liu, C. Yang, H. Xu, X. Li, H. Cui, *Vacuum* 77 (2004) 57
- 194]** R. Ghosh, G. K. Paul, D Basak, *Mater. Res. Bull.* 40 (2005) 1905
- 195]** S. Kobayashi, K. Oshima, T. Sasaki, N. Tsuboi, F. Kaneko, *Jpn. J. Appl. Phys.* 44 (2005) 1372
- 196]** O. F. Z. Khan, P. O'Brien, *Thin Solid Film* 173 (1989) 95
- 197]** M. Purica, E. Budianu, E. Rusu, M. Danila, R. Gavrilă, *Thin Solid Film* 403-404 (2002) 485
- 198]** V. Sallet, C. Thiandoume, J. F. Rommeluere, A. Lusson, A. Rivière, J. P. Rivière, O. Gorochoy, R. Triboulet, V. Muñoz-Sanjosed, *Mater. Lett.* 53 (2002) 126
- 199]** B. Hahn, G. heindel, E. P. Schoberer, W. Gebhardt, *Semicond. Sci. Technol.*, 13 (1998) 788
- 200]** H. Shen, M. Wraback, J. Pamulapati, S. Liang, C. Gorla, Y. Lu *Proc. Symposium*, Boston, MA, USA, 1998
- 201]** G. Du, J. Wang, X. Wang, X. Jiang, S. Yang, Y. Ma, W. Yan, D. Gao, X. Liu, H. Cao, J. Xu, R. P. H. Chang, *Vacuum* 69 (2003) 473
- 202]** N. F. Cooray, K. Kushiya, A. Fujimakaki, I. Sugiyama, T. Miura, D. Okumura, M. Sato, M. Ooshita, O. Yamase, *Sol. Energy Mater. Sol. Cell* 49 (1997) 291

203] N. W. Emanetoglu, C. Gorla, Y. Liu, S. Liang, Y. Lu, Mater. Sci. Semicond. Proc. 2 (1999) 247
